ELSEVIER

Journal of Volcanology and Geothermal Research 113 (2002) 379–389

Journal of volcanology and geothermal research

www.elsevier.com/locate/jvolgeores

Detecting volcanic eruption precursors: a new method using gravity and deformation measurements

Glyn Williams-Jones *, Hazel Rymer

Volcano Dynamics Group, Department of Earth Sciences, The Open University, Walton Hall, Milton Keynes, UK

Received 21 January 2000; accepted 12 June 2000

Abstract

One of the fundamental questions in modern volcanology is the manner in which a volcanic eruption is triggered; the intrusion of fresh magma into a reservoir is thought to be a key component. The amount by which previously ponded reservoir magma interacts with a newly intruded magma will determine the nature and rate of eruption as well as the chemistry of erupted lavas and shallow dykes. The physics of this interaction can be investigated through a conventional monitoring procedure that incorporates the simple and much used Mogi model relating ground deformation (most simply represented by Δh) to changes in volume of a magma reservoir. Gravity changes (Δg) combined with ground deformation provide information on magma reservoir mass changes. Our models predict how, during inflation, the observed $\Delta g/\Delta h$ gradient will evolve as a volcano develops from a state of dormancy through unrest into a state of explosive activity. Calderas in a state of unrest and large composite volcanoes are the targets for the methods proposed here and are exemplified by Campi Flegrei, Rabaul, Krafla, and Long Valley. We show here how the simultaneous measurement of deformation and gravity at only a few key stations can identify important precursory processes within a magma reservoir prior to the onset of more conventional eruption precursors.

Keywords: volcano; magma physics; micro-gravity; deformation; caldera; eruption triggers

1. Introduction

Explosive volcanic eruptions are often initiated by magma intrusion into a pre-existing magma reservoir (cf. Sparks et al., 1977; Pallister et al., 1992). The degree of interaction between the intruding magma and the pre-existing reservoir will determine the nature and rate of eruption as well as the chemistry of erupted lavas and shallow dykes. To understand the process therefore requires information on the physical and chemical processes occurring at depth within the magma reservoir. The majority of geophysical techniques, however, focus on shallow processes within the volcanic edifice. Micro-gravity monitoring, for example, has been used at numerous active volcanoes in order to identify the relatively shallow processes occurring within the feeder conduit (cf. Eggers and Chavez, 1979; Johnson et al., 1980; Yokoyama, 1989; Rymer and Brown, 1989; Berrino et al., 1992; Rymer et al., 1998b). The con-

* Corresponding author. Fax: +44-1908-655-151.
E-mail addresses: g.williams-jones@open.ac.uk (G. Williams-Jones), H.Rymer@open.ac.uk (H. Rymer).

0377-0273/02/$ – see front matter
PII: S0377-0273(01)00272-4

ventional micro-gravity survey involves repeated measurements of gravity change (Δg) and deformation (Δh) at a network of stations in and around the active crater or caldera (Rymer, 1994; Rymer et al., 1998b). The recent deaths of some well-known volcanologists (cf. Baxter and Gresham, 1997; Fujii and Nakada, 1999) emphasise the need to monitor volcanoes at a safe distance from the active centre. This, however, can often lead to reduced data quality. Here we discuss a new approach, first proposed by Rymer and Williams-Jones (2000), which actually benefits from gravity and deformation measurements made up to 6 km from the centre of activity. Physical processes deep within the magma reservoir, which can occur months to years before conventional precursors, can now be interpreted from $\Delta g/\Delta h$ gradients measured at a safe distance from the central volcanic edifice. This is exemplified by important examples from the calderas of Campi Flegrei, Rabaul, Krafla, and Long Valley, examined below.

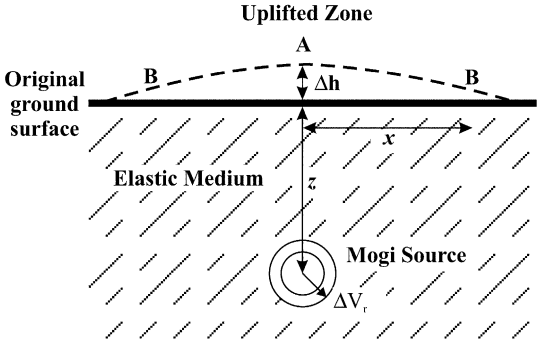

Fig. 1. A Mogi-type magma reservoir modelled in an elastic half space. The largest ground deformation changes (Δh) are observed in zone A. Measurable effects are also seen at some distance (x) from the centre of activity, such as at B. Using the measured or estimated values of the elastic properties of the country rock and the amount of ground deformation allows for the estimation of the change in volume of the sub-surface magma reservoir (ΔV_r). Small changes in gravity (Δg) may also be observed at these points (A and B) and when combined with ground deformation data, one can quantify the change in sub-surface magma mass (ΔM_m). Modified after Rymer and Williams-Jones (2000).

2. Gravity and height correlations

Conventional gravity and deformation data are usually modelled in terms of either a sphere or a Bouguer slab. Both are mathematically simple to model. To a first approximation, a magma reservoir can usually be most realistically modelled as a spherical body. If the depth of the magma reservoir is large compared to its radius, the gravitational effect of the reservoir can be considered to be that of a point source (Rymer, 1994). The Mogi model (Mogi, 1958) quantifies the deformation at the surface caused by dilation of a point source in a homogeneous elastic half space. The deformation will depend on the amount of dilation and the elastic properties of the medium (Fig. 1). Using ground deformation measurement techniques such as the Global Positioning System (GPS), Synthetic Aperture Radar differential interferometry (DInSAR), altimetry or levelling (cf. Smith et al., 1989; Murray et al., 1995; Dixon et al., 1997; Avallone et al., 1999), the change in edifice volume (ΔV_e) of the volcano can be estimated by integrating the observed height changes over the area of deformation. Measured or estimated values for the elastic properties of the country rock along with the amount of ground deformation can then be used to estimate the change in volume of the sub-surface magma reservoir (ΔV_r) (McKee et al., 1989; Vasco et al., 1990; Dvorak and Mastrolorenzo, 1991; Wicks et al., 1998). However, the change in volume alone provides little information on the actual processes taking place within the magma reservoir. If, in addition, small variations in the acceleration due to gravity are monitored, the changes in sub-surface magma mass (ΔM_m) can be quantified (Berrino et al., 1992). Simultaneous gravity and deformation measurements can therefore provide an estimate of ΔM_m and ΔV_r in order that changes in the average density of the magma reservoir may be deduced.

Changes in gravity and elevation are normally inversely correlated. The amount by which gravity varies with elevation is given by the free air gradient (FAG). If there is no change in the density (ρ) of the magma reservoir, the amount by which gravity varies with elevation can be described by

the Bouguer-corrected free air gradient (BCFAG) of a spherical body. The $BCFAG_{spherical}$ can be calculated using the following relationship in which the result is in units of μGal m^{-1}:

$$BCFAG_{spherical} = FAG + \frac{4\pi G \times 10^8}{3}\rho \quad (1)$$

where G is the universal gravitational constant (6.67×10^{-11} N m^2 kg^{-2}) and ρ is in kg m^{-3}. The theoretical value for the FAG is −308.6 μGal m^{-1}. Terrain effects and Bouguer anomalies can cause this value to differ by up to 40% from its theoretical value (Rymer, 1994 and references therein). The actual gradient of the BCFAG, which will vary depending on the density assumed for the surrounding rock, ranges from −253 to −230 μGal m^{-1} for magma densities of 2000 to 2800 kg m^{-3}, respectively, assuming the theoretical FAG.

If at all possible, the actual FAG should always be measured at each station during a micro-gravity/deformation survey. This can easily be accomplished in the field by making measurements first at the surface and then some distance off the ground (e.g. ∼1 m using a levelling tripod), and then dividing the difference of the two sets of measurements (Δg) by the difference in elevation

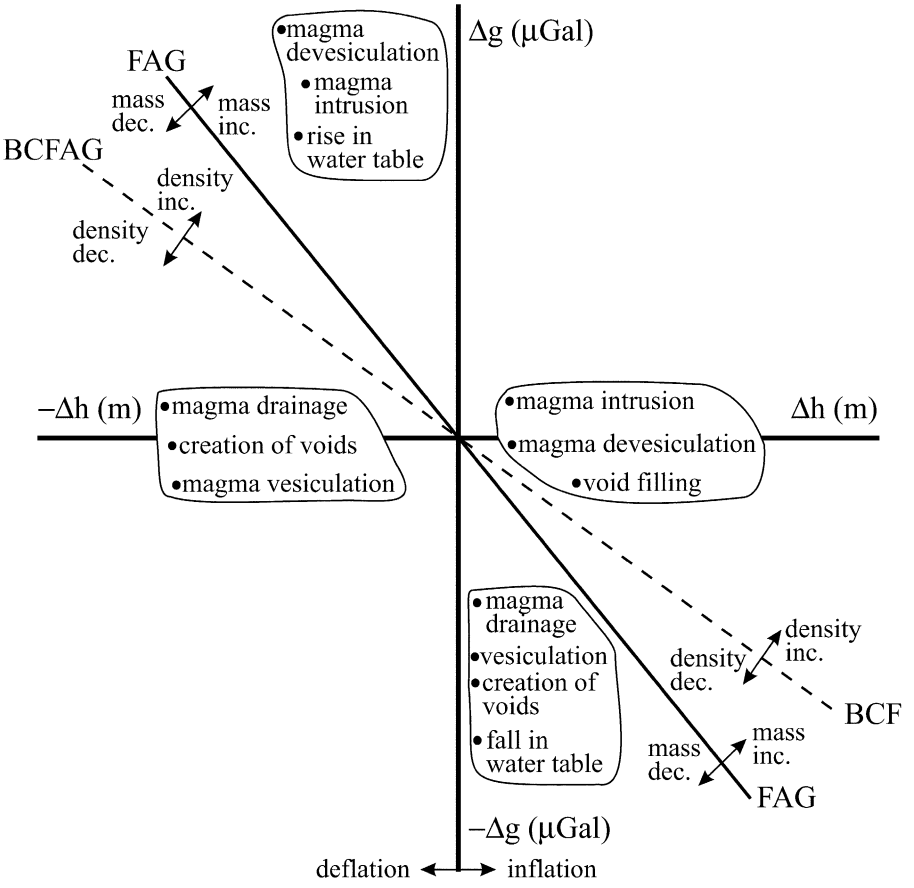

Fig. 2. Changes in gravity (Δg) and elevation (Δh) can be plotted in terms of $\Delta g/\Delta h$ gradients. When the gradient differs from the FAG, the variations are interpreted in terms of mass changes. Changes in density are shown by deviations from the BCFAG and FAG (−FAG+BCFAG). The theoretical FAG is commonly taken as −308.6 μGal m^{-1} but may vary by ∼40% depending on the local terrain and Bouguer anomaly. Assuming a Mogi point-source model and a theoretical FAG, the BCFAG may vary between −253 and −230 μGal m^{-1} for densities between 2000 and 2800 kg m^{-1}. Modified after Brown and Rymer (1991).

(Δh) (Berrino et al., 1984; Yokoyama, 1989; Rymer, 1994).

Gravity/elevation gradients are most easily visualised using a $\Delta g/\Delta h$ diagram (Fig. 2). $\Delta g/\Delta h$ gradients that deviate from the FAG are interpreted in terms of sub-surface mass changes. Data plotting above the FAG reflect mass increases while data plotting below it reflect mass decreases. Similarly, deviations from the BCFAG are interpreted as sub-surface density changes (Brown and Rymer, 1991; Berrino et al., 1992; Rymer et al., 1995). During periods of inflation, data plotting above the BCFAG reflect density increases, whereas data plotting below the BCFAG reflect density decreases. There is an important and intriguing region between the FAG and the BCFAG, in the lower right quadrant of Fig. 2, where during inflation there are mass increases and yet density decreases. Recognition of this is fundamental to understanding the physics of magma reservoir processes and the detection of eruption precursors (Fig. 3).

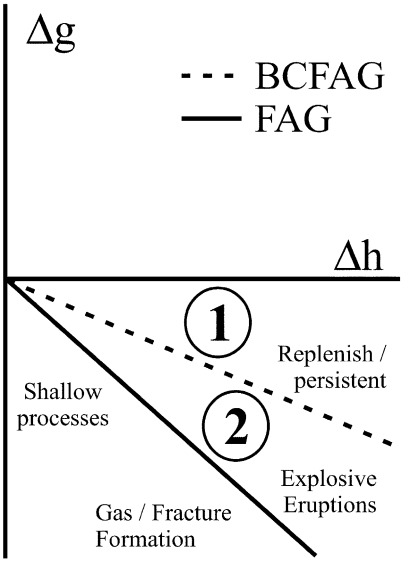

Fig. 3. During periods of inflation, increasing elevation (Δh) is accompanied by decreasing gravity (negative Δg), defined by the BCFAG. Region 1 represents anomalously large gravity increases and may be interpreted in terms of magma intrusion into a magma reservoir resulting in an increase in the average density of the reservoir. Region 2 reflects an overall density decrease and mass increase that may be interpreted in terms of gas build up within the magma reservoir, an important trigger mechanism for explosive eruptions. Data falling below the FAG and close to the Δg line may reflect shallow processes such as magma and gas fluctuations within the feeder conduit. Modified after Rymer and Williams-Jones (2000).

In order to investigate relatively shallow subsurface processes, micro-gravity and ground deformation surveys are commonly carried out in the region of maximum uplift, central to the volcanically active region (zone A, Fig. 1). However, sensitive instrumentation and techniques (e.g. Lacoste and Romberg or Scintrex gravity meters coupled with precise levelling or differential GPS) can detect small off axis variations ($\Delta g > 20$ μGal, $\Delta h > 1$ cm) at significant lateral distances (a few kilometres) from the active region (zone B, Fig. 1). Shallow volcanic events within the edifice (such as vesiculation and fracturing; (Rymer et al., 1998b), may be responsible for elevated 'noise' in the gravity data in region A. However, by making measurements away from the active centre, the signal-to-noise ratio of the data is significantly increased. Another potential source of uncertainty, the variation in groundwater levels, can be minimised in several ways; the seasonal variation may be reduced by making measurements at approximately the same time every year (Arnet et al., 1997) while the effects of water table fluctuations can be reduced by measuring at stations located on crystalline bedrock (Jachens and Roberts, 1985). The depth and distance at which it is possible to detect subtle changes within a Mogi-type magma reservoir can be calculated by solving for the total observed gravity change, Δg (μGal), in the following relationship (Dzurisin et al., 1980; Johnson, 1987; Eggers, 1987):

$$\Delta g = \left(\frac{\Delta M_{\mathrm{m}} \cdot G \cdot z}{(x^2 + z^2)^{3/2}} \right) \cdot 10^8 \qquad (2)$$

where ΔM_{m} is the change in sub-surface magma mass, G is the universal gravitational constant (6.672×10^{11} N m^2 kg^{-2}), x is the surface distance (m) out from the centre of the Mogi source, and z is the depth (m) to the Mogi point source (Fig. 1). Thus, for sub-surface magma mass changes of 10^{11} kg (e.g. Rabaul, Campi Flegrei; McKee et

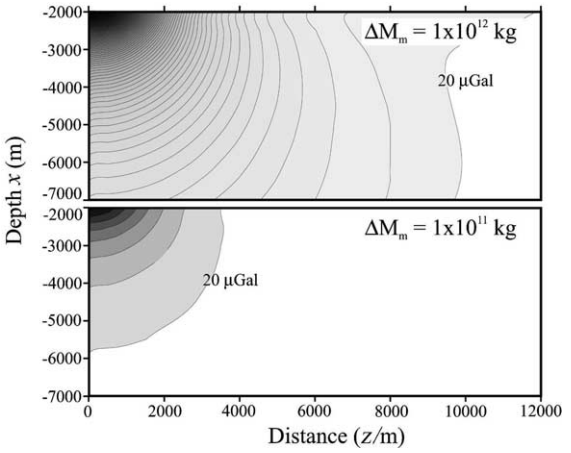

Fig. 4. The depth and distance at which it is possible to measure gravity changes (Δg) within a Mogi source can be determined for given changes in sub-surface magma mass (Eq. 2). For mass changes on the order of 10^{11} kg (similar to those of Campi Flegrei and Rabaul calderas), small gravity changes (>20 μGal) can be measured at horizontal distances of up to $\sim$4 km. For larger changes, e.g., 10^{12} kg, variations in gravity could be measured at up to 10 km from the centre of activity. Contours are 20 μGal. Depth (x) and distance (z) from the Mogi source are in metres (see Fig. 1).

al., 1989; Berrino et al., 1992, 1997) at a depth between 2 and 6 km, gravity variations (>20 μGal) can be measured at a horizontal distance of up to $\sim$4 km. For a mass change of the order of 10^{12} kg in a reservoir between 2 and 7 km deep, gravity changes are detectable at up to $\sim$10 km distance (Fig. 4).

3. Modelling a magma reservoir

Although the Mogi model represents a very simple magma reservoir, many published geophysical data are consistent with this type of source (Berrino et al., 1992; Arnet et al., 1997; Avallone et al., 1999). Here we present two end member models that illustrate how, by observing density changes within the magma reservoir, the hazard potential of a volcanic system can be determined.

An intruding magma with a relatively low Reynolds number (i.e. laminar flow; Sparks et al., 1980) will have little or no interaction with the surrounding magma reservoir (model 1, Fig. 5a). There will, however, be an overall mass increase in the system, measurable at the surface as a gravity increase along with limited ground deformation. This will result in a $\Delta g/\Delta h$ gradient that will plot between the BCFAG and the Δh axis (region 1) or along the BCFAG (Fig. 3) implying an overall density increase (region 1) or no density change (BCFAG) within the reservoir. Increasing density within a magma reservoir is often interpreted in terms of magma devesiculation and/or void filling (cf. Brown et al., 1991; Rymer, 1994). The dense intruded magma may be unable to rise and, in a closed system, the reservoir would eventually stagnate. However, if the magma pressure exceeds the local lithostatic pressure, dykes may be injected into the country rock and can in some cases eventually feed lava eruptions. The essential point here is that there is very limited interaction between the new intruding magma and the magma already in the reservoir. The mass increase is associated either with an overall density increase in the reservoir or in no density change. Either way, an eruption, and especially a large one, is unlikely.

At the other end of the spectrum, model 2 assumes a high Reynolds number (i.e. turbulent flow; Sparks et al., 1980) which will interact vigorously with the reservoir magma, heating it, causing convection, and therefore cooling the intruding magma (Fig. 5b; Eichelberger, 1980). This cooling can then lead to oversaturation and vesiculation (Huppert et al., 1982; Tait et al., 1989; Pallister et al., 1992), while superheating and decompression of the convecting reservoir magma may also cause volatile supersaturation and exsolution (Sparks et al., 1977). Consequent gravity and deformation variations would plot as a $\Delta g/\Delta h$ gradient between the FAG and BCFAG (region 2, Fig. 3) due to a net sub-surface mass increase and density decrease. Significantly, the interaction between the intruding magma and the older ponded magma is much more pervasive than in model 1. Magma mixing and mingling will cause significant bubble formation and the resulting increase in gas pressure within the reservoir is an essential pre-requisite to explosive eruptive activity (Eichelberger, 1980; Woods and Koyaguchi, 1994).

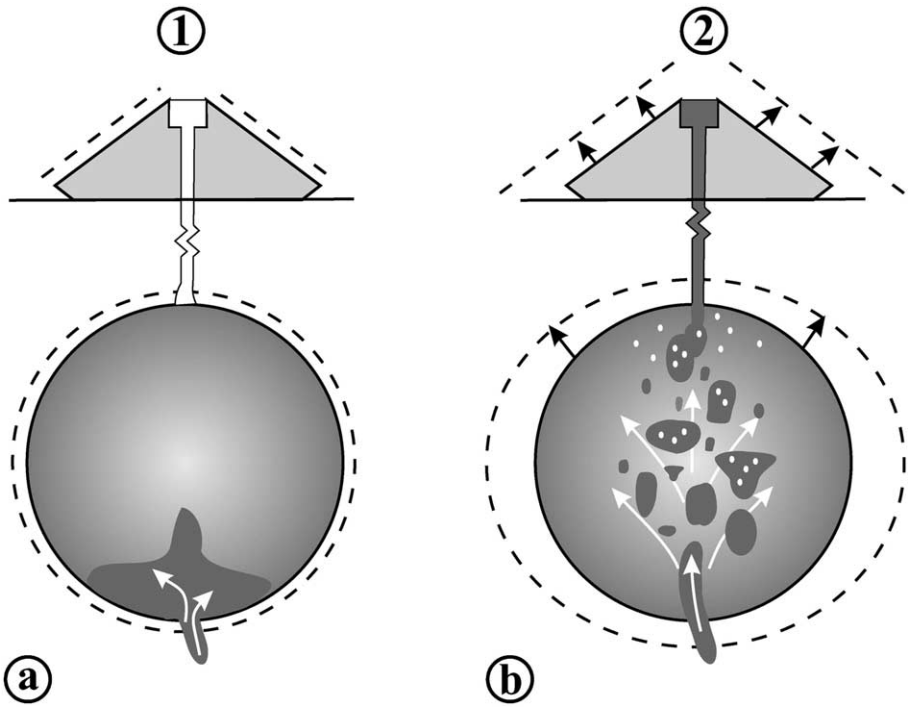

Fig. 5. (a) Model 1 depicts the intrusion of a low Reynolds number magma (i.e., laminar flow) into a magma reservoir. Importantly, there is little or no interaction with the surrounding magma. The observed $\Delta g/\Delta h$ gradient will fall into region 1 of Fig. 3. (b) Model 2 represents the other end member. Assuming an identical magma mass influx as model 1 but higher Reynolds number (i.e., turbulent flow), the intruding magma will interact vigorously with the surrounding magma, resulting in heating, convection, vesiculation and expansion of the reservoir. The observed gradient will fall into region 2 of Fig. 3. Modified after Rymer and Williams-Jones (2000).

These models suggest that the observed $\Delta g/\Delta h$ gradient will evolve as a volcano develops from a state of dormancy through unrest into explosive eruptive activity. The application of these models to hazard warning is as follows. As the gradient migrates from region 1 towards the BCFAG, the density of the magma reservoir decreases (Fig. 3) as a result of reduced crystallisation, increased buoyant melt and vesicle content. On the BCFAG, the magma reservoir volume increases but its density remains constant. In either scenario, eruption hazard is minimal. Once the measured $\Delta g/\Delta h$ gradient crosses the BCFAG, the density of the magma reservoir has decreased below the previous average value of the reservoir and the system becomes unstable. It is at this stage that the magma will be able to rise and presents an increased eruption hazard. If there is only limited heating, magma convection within the reservoir will follow; this has recently been linked with pulses of activity at the surface (Kazahaya et al., 1994; Stevenson and Blake, 1998). However, with excess heating, as gas pressure increases, the likelihood of an explosive eruption will increase (Woods and Koyaguchi, 1994).

4. Application of the models

Calderas in a state of unrest and large composite volcanoes are the most appropriate targets for the models proposed here. In an open volcanic system (i.e. one that displays persistent surface manifestations such as a stable lava lake, frequent explosive eruptions, etc.) gravity and deformation measurements made in region A (Fig. 1) will typ-

ically be dominated by shallow processes. Thus, in order to study processes within such a Mogi-type source, measurements must be made in region B, off the central axis of activity. A closed volcanic system on the other hand, generally has little or no surface activity allowing for $\Delta g/\Delta h$ gradient measurements to be made safely in both regions A and B. Some examples of these systems are presented below.

4.1. Campi Flegrei, Italy

The Campi Flegrei caldera (Naples, Italy) is a prime example of a persistently active closed system and a caldera in a state of unrest. Formed $\sim$35 000 years ago with the explosion of the Campanian Ignimbrite, the 12-km-diameter caldera last erupted in 1538. More recently, however, in the 1970s and early 1980s, the caldera was characterised by a bradyseismic crisis (an extended period of very slow vertical instability of the crust (Jackson, 1997) and a maximum uplift and gravity change of 1.616 m and -331 μGal, respectively. The measured FAG was -290 ± 5 μGal m^{-1} and assuming a point source density of 2500 km m^{-3}, the BCFAG was calculated to be -220 μGal m^{-1} (Berrino et al., 1992). The $\Delta g/\Delta h$ gradient during inflation was -213 ± 6 μGal m^{-1} and fell into region 1 (Fig. 6a) and as our model predicts, there was no eruption. In fact, between February 1981 and March 1983, the gradient actually evolved from the BCFAG towards the horizontal axis, well into region 1 (Fig. 3; Berrino, 1994). This episode was interpreted in terms of intrusion into a magma reservoir with a resulting overall sub-surface mass increase of $\sim 2 \times 10^{11}$ kg (Berrino et al., 1984). Mobilisation of the hydrothermal system has also been proposed as a possible cause of the observed uplift (Bonafede and Mazzanti, 1998).

Our model predicts that during inflation, once the $\Delta g/\Delta h$ gradient steepens beyond the BCFAG (-220 μGal m^{-1} in this case) into region 2, an explosive eruption is likely to follow. A modern explosive eruption of the same magnitude as the 1538 Pozzuoli eruption would affect an estimated 80 000, while 200 000 people would be at risk if the eruption was of similar magnitude to the larger 4400 yr BP Agnano-Monte Spina eruption (Barberi and Carapezza, 1996). Due to the extensive history of caldera unrest at Campi Flegrei and the increasing population of the Naples region, the need to distinguish between magma chamber processes (models 1 and 2, Fig. 5) is of critical importance to hazard mitigation.

4.2. Rabaul, Papua New Guinea

Another excellent example of a closed system is the Rabaul caldera (New Britain Island, Papua New Guinea) which has been in a state of unrest since at least the late 1800s. The caldera (14×9 km) lies within a shallow ignimbrite volcano and was modified by an earlier explosive episode 1400 years ago (Walker et al., 1981). In a more recent crisis (1973–1985), there was an overall uplift of $\sim$100 mm yr^{-1} with a maximum inflation of 1.8 m and gravity change of up to -410 μGal (McKee et al., 1989). Although no FAG was measured, given the amplitude and wavelength of a static Bouguer anomaly, the FAG has been estimated at -300 μGal (Berrino et al., 1992). Assuming a point source density of 2500 kg m^{-3}, the BCFAG was then calculated to be -239 μGal m^{-1} (Berrino et al., 1992). This episode was believed to have been caused by an intrusion of basic magma into a pre-existing reservoir that resulted in an overall sub-surface mass increase of 10^8 kg (McKee et al., 1989; Rymer, 1994). As at Campi Flegrei, the $\Delta g/\Delta h$ gradient (-216 ± 4 μGal m^{-1}) measured at Rabaul fell into region 1 (Fig. 6b); there was no eruption observed during this period. If the gradient were to have progressed below the BCFAG of -239 μGal m^{-1} (into region 2), our model predicts that an explosive eruption would have followed.

The most recent period of activity (1992–1999) which has been characterised by inflation and seismic swarms in fact developed into an extensive series of explosive and effusive eruptions. Petrological analyses of material erupted between 1997 and 1998 suggest that, as with the 1973–1985 crisis, current activity was initiated by the intrusion of new basaltic magma into the shallow dacitic reservoir (Bulletin of the Global Volcanism Network, 1992–1999). Unfortunately, no gravity data

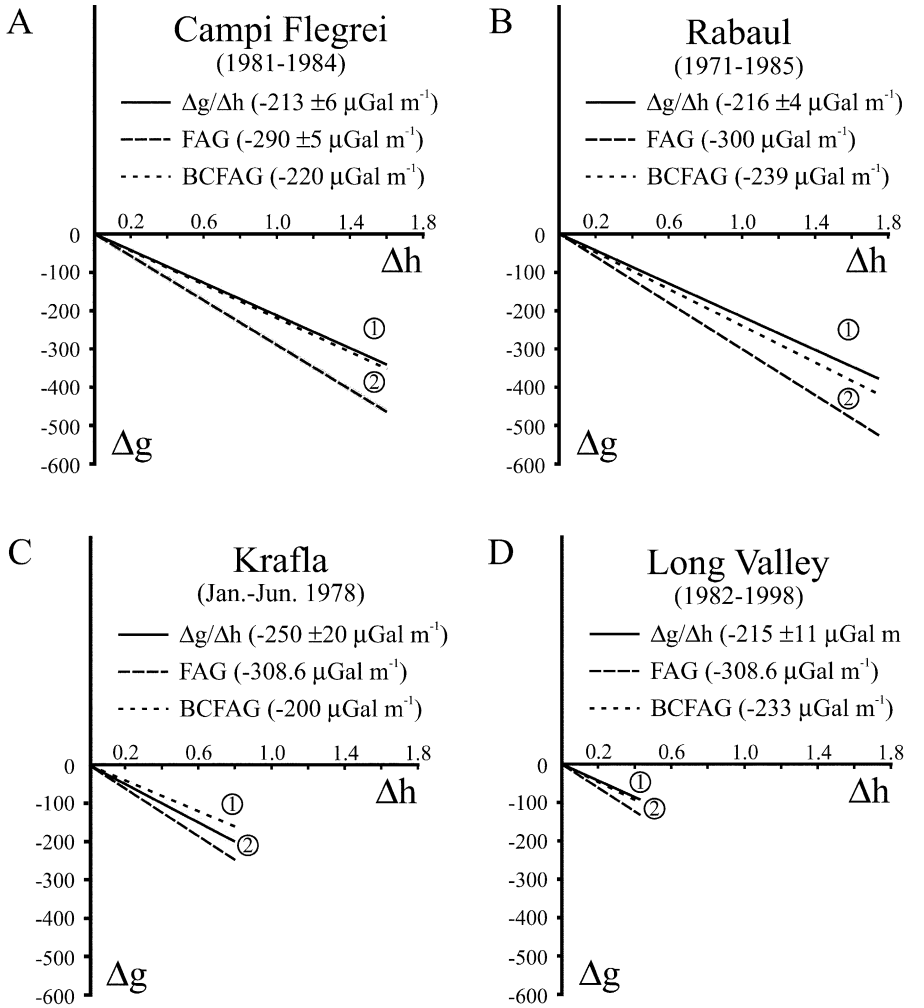

Fig. 6. The $\Delta g/\Delta h$ gradients observed during periods of inflation at the calderas of Campi Flegrei (A), Rabaul (B), Krafla (C), and Long Valley (D). The FAG and BCFAG gradients are measured or estimated/calculated values. Δh is in m and Δg in μGal. Grey shading represents estimated error for the measured gradients. Modified after Berrino et al. (1992).

are available for this period and thus it is not known whether the $\Delta g/\Delta h$ gradient had actually progressed into region 2 prior to the onset of eruptive activity (Fig. 6b). Although the town of Rabaul is not as densely populated as Naples, the activity at this centre poses a threat to the livelihood of tens of thousands of people. The population is well informed about volcanic activity and more than 50 000 were successfully and safely evacuated prior to the eruption in 1994 (Bulletin of the Global Volcanism Network, 1992–1999).

4.3. Krafla, Iceland

The Krafla caldera (northeast Iceland) is part of the large Krafla central volcano that straddles a 100-km-long N–S-trending fissure swarm. The 8×10-km caldera is believed to have formed $\sim$0.1 Myr ago during the last interglacial period with the explosive eruption of rhyolitic and dacitic rocks (Saemundsson, 1978). Krafla was last active during the 1975–1984 rifting episode that was characterised by lava extrusion, dyke emplacement and steady inflation interrupted by rapid

subsidence within the caldera. The inflationary periods are interpreted in terms of pressure increase within a shallow magma reservoir followed by rupture of the reservoir walls with rifting and dyke formation leading to rapid subsidence (Tryggvason, 1984). The January–June 1978 inflationary period was characterised by gravity and height variations which followed a gradient of -250 ± 20 μGal m^{-1} (Johnson et al., 1980). A FAG and a BCFAG for the caldera were calculated at -308.6 and -200 μGal m^{-1}, respectively (Rymer et al., 1998a). This is the only published example, where during inflation, the observed $\Delta g/\Delta h$ gradient fell into region 2 (Fig. 6c). Our model suggests that magma reservoir mass increase but density decrease is likely to lead to an eruption. In this basaltic extensional tectonic regime, fire fountaining occurred, feeding lava flows and there was also considerable dyke injection. Post-eruptive activity has been characterised by continued deflation (30 mm yr^{-1}; Sigmundsson et al., 1997) and a net gravity decrease caused mainly by the drainage of 4×10^{10} kg of magma (Rymer et al., 1998a). The hazard to the population is extremely small at this site. However Lake Myvatn, just a few kilometres away, is a very popular tourist centre and Krafla supports an industrial geothermal power plant so that eruptive activity affects thousands of people directly.

4.4. Long Valley, USA

Long Valley caldera (California, USA), which is located on the eastern edge of the Sierra Nevada tectonic block, formed 730 kyr ago during the Bishop Tuff eruption. This was followed shortly by the formation of a resurgent rhyolite dome (Bailey et al., 1976). A negative Bouguer anomaly, with a steep gradient >20 mGal in some places, is concentric with the caldera and reflects the lateral transition from low-density caldera material to the high-density crystalline rocks of the Sierra Nevadas (Kane et al., 1976; Jachens and Roberts, 1985). During the 1982–1998 inflationary period, centred on the resurgent dome, a gravity decrease of up to 107 ± 6 μGal and maximum residual inflation of 0.42 ± 0.05 m occurred, giving an average $\Delta g/\Delta h$ gradient of -215 ± 11 μGal m^{-1} (Dzurisin et al., 1990; Battaglia et al., 1999). This episode has most recently been interpreted in terms of a mass increase (3.8×10^{11} to 17.8×10^{11} kg) due to the intrusion of basaltic magma into a rhyolitic reservoir beneath the resurgent dome (Battaglia et al., 1999). Assuming the theoretical FAG and a density of 2700 kg m^{-3}, the calculated BCFAG is -233 μGal m^{-1} and as for some of the previous examples, the measured $\Delta g/\Delta h$ gradient falls above the BCFAG into region 1. Our model predicts that the net density of the reservoir will increase, thus making an eruption unlikely (Fig. 6d).

5. Conclusions

Large composite volcanoes and calderas in a state of unrest are appropriate targets at which to consider the models presented here, where they are characterised by a spherical Mogi-type source. Conventional micro-gravity surveys involve the measurement of a large network of stations, often in proximity to centres of volcanic activity, and inevitably focus on relatively shallow processes. Here, we require simultaneous measurements of deformation and gravity at only a few key stations off axis of the centre of activity. Clearly the number of stations required would depend on the individual circumstances and available instrumentation, but at 1 to 5, will be considerably less than required for conventional micro-gravity surveys. The advent of continuous gravity and deformation monitoring (cf. Berrino et al., 1997; Dixon et al., 1997) will allow for a dramatically increased temporal resolution by this method. The spatial resolution is not compromised badly, since the sources of interest in the proposed method are deeper than for conventional micro-gravity surveys. Very small changes in mass or density of a magma reservoir at depths of 2–7 km can be made at a safe distance (up to 10 km) from the active centre, greatly reducing the risk to scientists. By quantifying the magnitude and rate of these changes, eruption precursors within the reservoir may be detected well before the magma begins to rise towards the surface, offering significantly more time for hazard

mitigation and evacuation. Determining the nature of these processes is also critical for evaluating the potential magnitude of the hazard. Some 138 calderas have shown a degree of unrest in historical times (Newhall and Dzurisin, 1988) and about half the well-documented cases resulted in eruption. At silicic calderas, only 15% of the cases of unrest resulted in eruption, but increasing population and vulnerability to explosive eruptions means that a better understanding of caldera unrest is an essential goal for the new millennium.

Acknowledgements

This research was supported by the Royal Society, The Open University Research Development Fund and NERC. We thank J. B. Murray, C.A. Locke, J. Cassidy and D. Rothery for many useful discussions about this work. This work was greatly improved by the comments of an anonymous reviewer.

References

Arnet, F., Kahle, H.-G., Klingelé, E., Smith, R.B., Meertens, C.M., Dzurisin, D., 1997. Temporal gravity and height changes of the Yellowstone caldera, 1977–1994. Geophys. Res. Lett. 24, 2741–2744.

Avallone, A., Zollo, A., Briole, C., Delacourt, C., Beauducel, F., 1999. Subsidence of Campi Flegrei (Italy) detected by SAR interferometry. Geophys. Res. Lett. 26, 2303–2306.

Bailey, R.A., Dalrymple, G.B., Lanphere, M.A., 1976. Volcanism, structure and geochronology of Long Valley Caldera, Mono County, California. J. Geophys. Res. 81, 725–744.

Barberi, F., Carapezza, M.L., 1996. The problem of volcanic unrest: the Campi Flegrei case history. In: Scarpa, R., Tilling, R.I. (Eds.), Monitoring and Mitigation of Volcano Hazards. Springer, Berlin, pp. 771–786.

Battaglia, M., Roberts, C., Segall, P., 1999. Magma intrusion beneath Long Valley Caldera confirmed by temporal changes in gravity. Science 285, 2119–2122.

Baxter, P.J., Gresham, A., 1997. Deaths and injuries in the eruption of Galeras Volcano, Colombia, January 14, 1993. J. Volcanol. Geotherm. Res. 77, 325–338.

Berrino, G., 1994. Gravity changes induced by height-mass variations at the Campi Flegrei caldera. J. Volcanol. Geotherm. Res. 61, 293–309.

Berrino, G., Corrado, G., Luongo, G., Toro, B., 1984. Ground deformation and gravity changes accompanying the 1982 Pozzuoli uplift. Bull. Volcanol. 47, 187–200.

Berrino, G., Rymer, H., Brown, G.C., Corado, C., 1992. Gravity-height correlations for unrest at calderas. J. Volcanol. Geotherm. Res. 53, 11–26.

Berrino, G., Corrado, G., Magliulo, R., Umberto, R., 1997. Continuous record of the gravity changes at Mt. Vesuvius. In: Boschi, E. (Ed.), Special issue dedicated to Professor Michele Caputo on his seventieth birthday. Ann. Geofis. 40, 1019–1028.

Bonafede, M., Mazzanti, M., 1998. Modelling gravity variations consistent with ground deformation in the Campi Flegrei caldera (Italy). J. Volcanol. Geotherm. Res. 81, 137–157.

Brown, G.C., Rymer, H., 1991. Microgravity monitoring at active volcanoes: a review of theory and practice. Cahier Cent. Eur. Géodyn. Séismol. 4, 279–304.

Brown, G.C., Rymer, H., Stevenson, D., 1991. Volcano monitoring by microgravity and energy budget analysis. J. Geol. Soc. London 148, 585–593.

Bulletin of the Global Volcanism Network, 1992–1999. Rabaul. Smithsonian Institution, 17:05–24:10 (http://www.volcano.si.edu/gvp/volcano/region05/newbrit/rabaul/var.htm).

Dixon, T.H., Mao, A., Bursik, M., Heflin, M., Langbein, J., Stein, R., Webb, F., 1997. Continuous monitoring of surface deformation at Long Valley Caldera, California, with GPS. J. Geophys. Res. 102, 12017–12034.

Dvorak, J., Mastrolorenzo, G., 1991. The mechanisms of recent vertical crustal movements in Campi Flegrei caldera. Spec. Pap. Geol. Soc. Am. 263, 47.

Dzurisin, D., Anderson, L.A., Eaton, G.P., Koyanagi, R.Y., Lipman, P.W., Lockwood, J.P., Okamura, R.T., Puniwai, G.S., Sako, M.K., Yamashita, K.M., 1980. Geophysical observations of Kilauea volcano, Hawaii, 2. Constraints on the magma supply during November 1975–September 1977. J. Volcanol. Geotherm. Res. 7, 241–269.

Dzurisin, D., Savage, J.C., Fournier, R.O., 1990. Recent crustal subsidence at Yellowstone caldera, Wyoming. Bull. Volcanol. 52, 247–270.

Eggers, A.A., 1987. Residual gravity changes and eruption magnitudes. In: Williams, S.N., Carr, M.J. (Eds.), Richard E. Stoiber 75th Birthday Volume. J. Volcanol. Geotherm. Res. 33, 201–216.

Eggers, A.A., Chavez, D., 1979. Temporal gravity variations at Pacaya volcano, Guatemala. J. Volcanol. Geotherm. Res. 6, 391–402.

Eichelberger, J.C., 1980. Vesiculation of mafic magma during replenishment of silic magma reservoirs. Nature 288, 446–450.

Fujii, T., Nakada, S., 1999. The 15 September 1991 pyroclastic flows at Unzen Volcano (Japan): a flow model for associated ash-cloud surges. J. Volcanol. Geotherm. Res. 89, 159–172.

Huppert, H.E., Sparks, R.S.J., Turner, J.S., 1982. Effects of volatiles on mixing in calc-alkaline magma systems. Nature 297, 554–557.

Jachens, R.C., Roberts, C.W., 1985. Temporal and areal gravity investigations at Long Valley Caldera, California. J. Geophys. Res. 90, 11210–11218.

Jackson, J.A. (Ed.), 1997. Glossary of Geology, 4th edn., American Geological Institute, Alexandria, VA, 769 pp.

Johnson, D.J., 1987. Elastic and inelastic magma storage at Kilauea Volcano. In: Decker, R.W., Wright, T.L., Stauffer, P.H. (Eds.), Volcanism in Hawaii. U.S. Geol. Surv. Prof. Pap. 1350, pp. 1297–1306.

Johnson, G.V., Björnsson, A., Sigurdsson, S., 1980. Gravity and elevation changes caused by magma movement beneath the Krafla caldera, Northeast Iceland. J. Geophys. Res. 47, 132–140.

Kane, M.F., Mabey, D.R., Brace, R.L., 1976. A gravity and magnetic investigation of the Long Valley caldera, Mono County, California. J. Geophys. Res. 81, 754–762.

Kazahaya, K., Shinohara, H., Saito, G., 1994. Excessive degassing of Izu-Oshima volcano: magma convection in a conduit. Bull. Volcanol. 56, 207–216.

McKee, C., Mori, J., Talai, B., 1989. Microgravity changes and ground deformation at Rabaul caldera, 1973–1985. In: Latter, J.H. (Ed.), Volcanic Hazards: Assessment and Monitoring. IAVCEI Proceedings in Volcanology 1. Springer, Berlin, pp. 399–428.

Mogi, K., 1958. Relations between the eruptions of various volcanoes and the deformations of the ground surfaces around them. Bull. Earthquake Res. Inst. 36, 99–134.

Murray, J.B., Pullen, A.D., Saunders, S., 1995. Ground deformation surveying of active volcanoes. In: McGuire, B., Kilburn, C.R.J., Murray, J. (Eds.), Monitoring Active Volcanoes. UCL Press, London, pp. 113–150.

Newhall, C.G., Dzurisin, D., 1988. Historical unrest at large calderas of the world. U.S. Geol. Surv. Bull. 1855, 1108.

Pallister, J.S., Hoblitt, R.P., Reyes, A.G., 1992. A basalt trigger for the 1991 eruptions of Pinatubo volcano. Nature 356, 426–428.

Rymer, H., 1994. Microgravity change as a precursor to volcanic activity. J. Volcanol. Geotherm. Res. 61, 311–328.

Rymer, H., Brown, G.C., 1989. Gravity changes as a precursor to volcanic eruptions at Poás volcano, Costa Rica. Nature 342, 902–905.

Rymer, H., Cassidy, J., Locke, C.A., Murray, J.B., 1995. Magma movements in Etna volcano associated with the major 1991–1993 lava eruption: evidence from gravity and deformation. Bull. Volcanol. 57, 451–461.

Rymer, H., Cassidy, J., Locke, C.A., Sigmundsson, F., 1998. Post-eruptive gravity changes from 1990 to 1996 at Krafla, Iceland. J. Volcanol. Geotherm. Res. 87, 141–149.

Rymer, H., van Wyk de Vries, B., Stix, J., Williams-Jones, G., 1998. Pit crater structure and processes governing persistent activity at Masaya Volcano, Nicaragua. Bull. Volcanol. 59, 345–355.

Rymer, H., Williams-Jones, G., 2000. Volcanic eruption prediction: magma chamber physics from gravity and deformation measurements. Geophys. Res. Lett. 27, 2389–2392.

Saemundsson, K., 1978. Fissure swarms and central volcanoes of the neo-volcanic zones of Iceland. Geol. J. Spec. Issue 10, 415–432.

Sigmundsson, F., Vadon, H., Massonnet, D., 1997. Readjustment of the Krafla spreading segment to crustal rifting measured by satellite radar interferometry. Geophys. Res. Lett. 24, 1843–1846.

Smith, R.B., Reilinger, R.E., Meertens, C.M., Hollis, J.R., Holdahl, S.R., Dzurisin, D., Gross, W.K., Klingele, E.E., 1989. What's moving at Yellowstone? The 1987 crustal deformation survey from GPS, levelling, precision gravity, and trilateration. EOS Trans. Am. Geophys. Union 70, 113–125.

Sparks, R.S.J., Meyer, P., Sigurdsson, H., 1980. Density variation amongst Mid-Ocean Ridge basalts: implications for magma mixing and the scarcity of primitive lavas. Earth Planet. Sci. Lett. 46, 419–430.

Sparks, S.R.J., Sigurdsson, H., Wilson, L., 1977. Magma mixing: a mechanism for triggering acid explosive eruptions. Nature 267, 315–318.

Stevenson, D.S., Blake, S., 1998. Modelling the dynamics and thermodynamics of volcanic degassing. Bull. Volcanol. 60, 307–317.

Tait, S., Jaupart, C., Vergniolle, S., 1989. Pressure, gas content and eruption periodicity of a shallow, crystallising magma chamber. Earth Planet. Sci. Lett. 92, 107–123.

Tryggvason, E., 1984. Widening of the Krafla fissure swarm during the 1975–1981 volcano-tectonic episodes. Bull. Volcanol. 47, 47–69.

Vasco, D.W., Smith, R.B., Taylor, C.L., 1990. Inversion for sources of crustal deformation and gravity change at the Yellowstone caldera. J. Geophys. Res. 95, 19839–19856.

Walker, G.P.L., Heming, R.F., Sprod, T.J., Walker, H.R., 1981. Latest major eruptions of Rabaul volcano. In: Johnson, R.W. (Ed.), Cooke-Ravian Volume of Volcanological Papers. Geol. Surv. Papua New Guinea 10, 81–193.

Wicks, C., Thatcher, W., Dzurisin, D., 1998. Migration of fluids beneath Yellowstone caldera inferred from satellite radar interferometry. Science 282, 458–462.

Woods, A.W., Koyaguchi, T., 1994. Transitions between explosive and effusive eruptions of silicic magmas. Nature 370, 641–644.

Yokoyama, I., 1989. Microgravity and height changes caused by volcanic activity: four Japanese examples. Bull. Volcanol. 51, 333–345.